Localization accuracy from automatic and semi-automatic rigid registration of locally-advanced lung cancer targets during image-guided radiation therapy

Scott P. Robertson, Elisabeth Weiss, and Geoffrey D. Hugo[a)]
Department of Radiation Oncology, Virginia Commonwealth University, Richmond, Virginia 23298

(Received 19 July 2011; revised 29 November 2011; accepted for publication 1 December 2011; published 21 December 2011)

Purpose: To evaluate localization accuracy resulting from rigid registration of locally-advanced lung cancer targets using fully automatic and semi-automatic protocols for image-guided radiation therapy.
Methods: Seventeen lung cancer patients, fourteen also presenting with involved lymph nodes, received computed tomography (CT) scans once per week throughout treatment under active breathing control. A physician contoured both lung and lymph node targets for all weekly scans. Various automatic and semi-automatic rigid registration techniques were then performed for both individual and simultaneous alignments of the primary gross tumor volume (GTV_P) and involved lymph nodes (GTV_{LN}) to simulate the localization process in image-guided radiation therapy. Techniques included "standard" (direct registration of weekly images to a planning CT), "seeded" (manual prealignment of targets to guide standard registration), "transitive-based" (alignment of pretreatment and planning CTs through one or more intermediate images), and "rereferenced" (designation of a new reference image for registration). Localization error (LE) was assessed as the residual centroid and border distances between targets from planning and weekly CTs after registration.
Results: Initial bony alignment resulted in centroid LE of 7.3 ± 5.4 mm and 5.4 ± 3.4 mm for the GTV_P and GTV_{LN}, respectively. Compared to bony alignment, transitive-based and seeded registrations significantly reduced GTV_P centroid LE to 4.7 ± 3.7 mm ($p = 0.011$) and 4.3 ± 2.5 mm ($p < 1 \times 10^{-3}$), respectively, but the smallest GTV_P LE of 2.4 ± 2.1 mm was provided by rereferenced registration ($p < 1 \times 10^{-6}$). Standard registration significantly reduced GTV_{LN} centroid LE to 3.2 ± 2.5 mm ($p < 1 \times 10^{-3}$) compared to bony alignment, with little additional gain offered by the other registration techniques. For simultaneous target alignment, centroid LE as low as 3.9 ± 2.7 mm and 3.8 ± 2.3 mm were achieved for the GTV_P and GTV_{LN}, respectively, using rereferenced registration.
Conclusions: Target shape, volume, and configuration changes during radiation therapy limited the accuracy of standard rigid registration for image-guided localization in locally-advanced lung cancer. Significant error reductions were possible using other rigid registration techniques, with LE approaching the lower limit imposed by interfraction target variability throughout treatment. [DOI: 10.1118/1.3671929]

Key words: non-small cell lung cancer, lymph nodes, image registration, image-guided radiation therapy

I. INTRODUCTION

One of the major limitations in lung cancer radiotherapy involves the localization of targets before and during a treatment fraction.[1] Geometric uncertainties inherent in the preparation and execution of each fraction are typically mitigated by the use of treatment margins to ensure that target coverage is maintained to within a clinically acceptable probability.[2] Improving target localization will therefore decrease the size of treatment margins and spare an increased volume of healthy tissue from irradiation.[3] This increases the potential for dose escalation,[4] which has been shown in numerous studies to increase local tumor control and ultimately lead to better patient outcomes.[5,6]

Image-guided radiotherapy has become a widespread clinical tool[7] with numerous applications to the treatment process,[8] one of which includes patient setup. Three-dimensional and even four-dimensional pretreatment imaging techniques facilitate substantially better target localization than traditional guidance practices, such as the use of in-room lasers or planar portal imaging.[9,10] With these older methods, patient setup was generally accomplished by aligning external surrogates or bony-anatomy.[11] However, the correlation between these features and lung cancer targets may be poor.[12–14] Pretreatment volumetric imaging provides superior visualization of internal anatomy and makes possible the use of soft-tissue surrogates,[15–17] although these features may also fail to correlate with the position and motion of lung cancer targets.[5,18]

In theory, direct registration of targets should provide optimal localization,[19] but this strategy presents difficulties as well. Significant pathological changes are possible throughout treatment, including lung tumor regression[20–24] and changes in metastatic nodal volume.[10,25] In addition, pathology of the ipsilateral lung such as pleural effusion and atelectasis (which we term "pathology-induced changes") can alter the local environment surrounding lung cancer targets.[4] Finally, the configuration between primary tumors and lymph nodes may change over time due to intertarget variability.[18,25,26] These effects complicate manual target alignment and the use of rigid registration algorithms.[24,26] Deformable registration may be better suited to address moderate pathological and pathology-induced changes, but substantial variation throughout treatment may lead to misregistration.[27] Furthermore, validation of deformable algorithms is not yet available for the setup of lung cancer patients, and relatively long computation times have inhibited clinical implementation to date for patient setup.[28] As a result of the limitations of deformable registration, and because rigid registration is the current clinical standard for image-guided radiation therapy, we set out to assess the performance and limitations of rigid registration algorithms for the setup of lung cancer patients. The purpose of this study was to evaluate localization error resulting from automatic rigid registration applied directly to the alignment of primary lung tumors and involved lymph nodes. The secondary purpose was to develop and evaluate practical adaptations of this rigid registration protocol to reduce the residual localization error.

II. METHODS

II.A. Patient population

Seventeen patients with stage IIA to IV locally-advanced non-small cell lung cancer received weekly computed tomography (CT) scans under active breathing control according to a protocol approved by the local institutional review board. Details of the imaging protocol were described by Glide-Hurst *et al.*[29] Briefly, all patients completed an initial coaching session on the Active Breathing Coordinator (version 2.0, Elekta, Stockholm, Sweden). Breath-holds were conducted at 80% of the end-of-normal inspiration lung volume for 8–15 s. Patient characteristics are summarized in Table I.

II.B. Image acquisition

Weekly CT images were acquired without contrast using a 16-slice helical CT scanner (Brilliance Big Bore, Philips Medical Systems, Andover, MA). Four to seven imaging sessions were completed for each patient throughout treatment, for a total of 99 images. The week 1 planning CT was designated as the reference image, R, and all other weekly CTs were designated as secondary images, S_n, for registration. To eliminate patient setup uncertainties, each secondary image was manually translated and rotated to match the bony-anatomy of the reference CT [Figs. 1(a) and 1(b)] in a research version of the PINNACLE[3] treatment planning system (version 8.1y, Philips Medical Systems, Fitchburg, WI). The gross tumor volume (GTV) was contoured by a physician for all lung cancer targets, including primary tumors (GTV_P) and metastatic lymph nodes (GTV_{LN}). For patients with multiple targets of each type, the final GTV_P and GTV_{LN} were defined as the union of all contoured primary tumors and involved lymph nodes, respectively. Bony alignment error was defined as the centroid and border displacements between corresponding targets from R and S_n in this initial alignment.

TABLE I. Population characteristics.

Description	Treatment target	
	Primary tumor	Lymph nodes
Total number of patients	17	14
With pathology-induced changes		
Atelectasis	5	5
Pleural effusion	2	2
Number of patients with:		
1 Contoured target	16	9
2 Contoured targets	1	4
3 Contoured targets	0	1
Number of imaging sessions	4–7	4–7
Total number of CT scans	99	83
Number of registrations	82	69
Target volume:		
Average ± St dev (cm^3)	67.8 ± 83.0	5.7 ± 7.2
Range (cm^3)	0.4–377.4	0.2–27.0
Change per week[a]	−7.6% ($R^2 = 0.28$, $p < 1 \times 10^{-6}$)	−6.5% ($R^2 = 0.17$, $p < 1 \times 10^{-3}$)

[a]As determined from linear regression between normalized tumor volume (relative to week 1 for each patient) and treatment week.

II.C. Individual target registration

Table II lists the registration strategies evaluated in this study. We first explored "standard" registration of all secondary images to the planning CT in the PINNACLE[3] treatment planning system. Automatic, intensity-based rigid registrations were used to directly align the treatment targets from each S_n to R [Figs. 1(c) and 1(d)]. The registration volume on R was limited to either the GTV_P or GTV_{LN} plus a uniform 1 cm margin, which was found in initial tests to provide the best target localization compared to other margin sizes. No volume limits were applied to S_n to avoid potentially cropping the secondary target, which was assumed to be uncontoured and unknown *a priori* on weekly images. Only translational degrees of freedom were performed to simulate shifts in the treatment couch. Separate registrations were performed for the GTV_P and GTV_{LN} using each of the available algorithms in PINNACLE:[3] local correlation, cross correlation, and normalized mutual information (NMI). Localization error (LE) was computed as the residual displacement between manually-delineated targets from R and S_n after automatic registration. To address instances of large residual LE from standard registration, a "seeded" registration strategy was also explored in which secondary images were

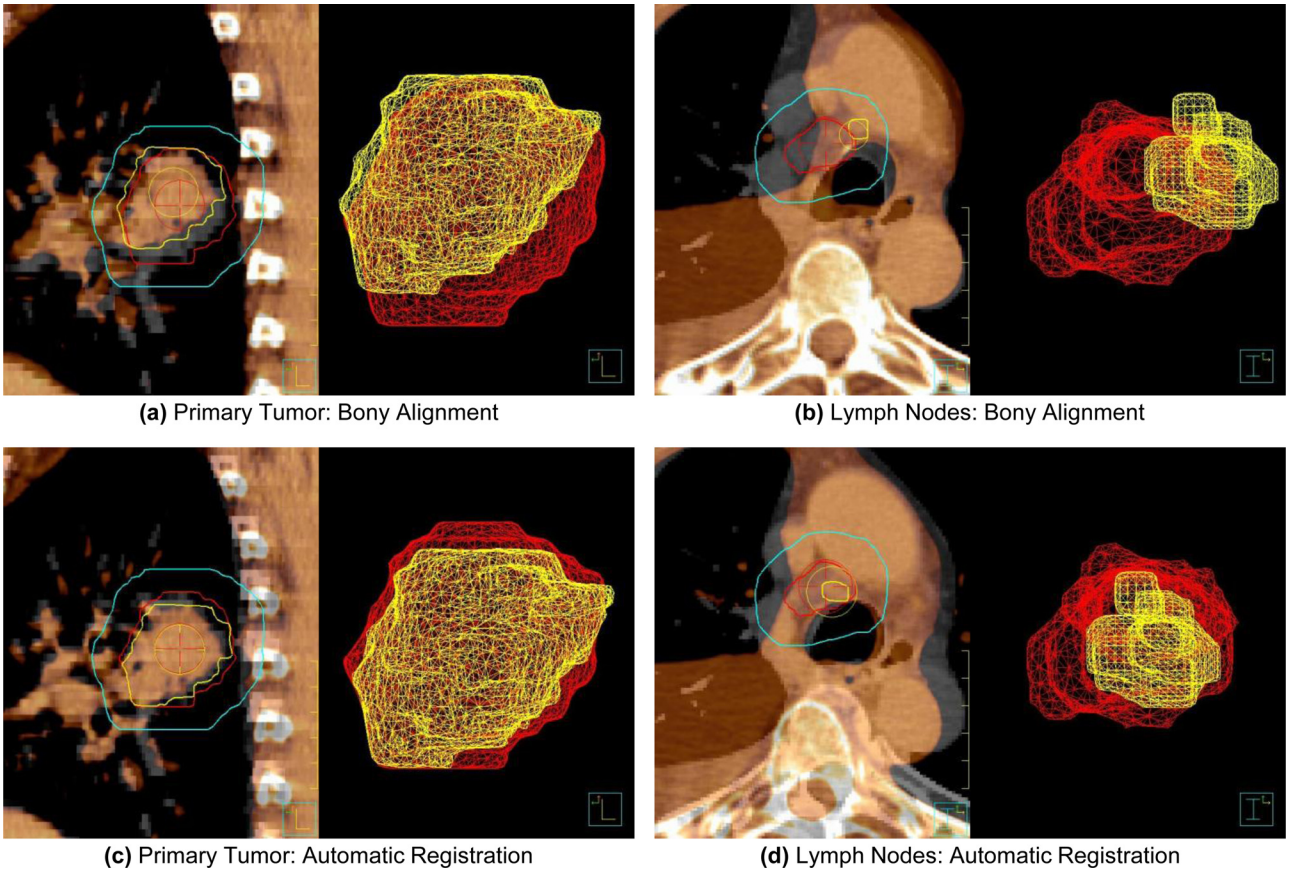

FIG. 1. Overlay image showing the registration of targets from reference and secondary CTs from two different patients. Images were initially aligned using bony-anatomy (a)–(b). Pleural effusion likely contributed to the initial misalignment of an involved lymph node in (b). Automatic, rigid registration improved the localization of both the primary tumor (c) and involved lymph nodes (d) for patients in this study. The smaller surface meshes (foreground) represent targets from weekly CT images, whereas the larger surface meshes (background) represent targets from the initial planning CT. An additional contour is provided to demonstrate the registration volume obtained by a 10 mm isotropic expansion of targets from the planning CT.

brought into better initial alignment to guide standard registration. Specifically, secondary images were manually translated to align the centroids of planning and weekly target volumes to reduce the impact of large initial displacements on the accuracy of automatic registration. Because seeded registration required a manual pre-alignment of targets, it was considered a semi-automatic localization strategy.

Further reductions in target LE were sought by mitigating the gradual but sometimes substantial deformations observed throughout treatment, including both pathological and pathology-induced changes. This was accomplished using a "transitive-based" (TB) registration technique similar to that explored by Škrinjar *et al.*[30] Briefly, any two images in a sequence (e.g., R and S_n) can be registered by matching each to an arbitrary intermediate image, S_m, where $1 < m < n$ for the present study. According to the transitivity property,[30] the registration between S_n and R should be equal to the composition of intermediate registrations

$$\mathbf{T}(S_n \rightarrow R) = \mathbf{T}(S_m \rightarrow R) \circ \mathbf{T}(S_n \rightarrow S_m), \tag{1}$$

where $\mathbf{T}(A \rightarrow B)$ is the transformation resulting from registration of image A to image B, and $\circ$ denotes the composition of two separate registrations. In general, CT scans acquired with fewer fractions between them demonstrated less substantial deformation of internal anatomy. Transitive-based registrations were therefore expected to achieve lower LE than standard registrations as long as the composition of intermediate steps did not propagate target LE substantially.

Two subtypes of TB registration were explored, termed "intermediate" and "consecutive." Intermediate-TB registration involved the alignment of all weekly images acquired during or after the fourth week of treatment to the week 3 CT, S_3. This result, in turn, was composed with the registration between S_3 and R, or

$$\mathbf{T}^{TB}_{\text{intermed}}(S_n \rightarrow R) = \begin{cases} \mathbf{T}(S_3 \rightarrow R) \circ \mathbf{T}(S_n \rightarrow S_3) & 3 < n \\ \mathbf{T}(S_n \rightarrow R) & 1 < n \leq 3 \end{cases}. \tag{2}$$

The week 3 CT was designated as the sole intermediate image for several reasons. Underberg *et al.* showed that significant target volume regression was possible by the fourth week of treatment.[31] Similarly, Woodford *et al.* observed that adaptive planning is most beneficial for targets regressing by at least 30% within the first 20 fractions.[32] Although adaptive planning was not considered in this study, the week 3 CT was still hypothesized to provide reasonable localization accuracy between targets from intermediate and reference images, while enabling reasonable registration of all subsequent weekly images that may be subject to these large

TABLE II. Summary of nine registration techniques explored in this study. The nominal techniques provide a lower bound on LE for each metric. As such, it is unnecessary to compute border LE for centroid alignment and centroid LE for border alignment. Therefore, only eight registration techniques are presented for each LE metric in the remaining tables and in Figs. 3–6. NMI: normalized mutual information.

Registration	Short name	Description	Implementation
Bony-anatomy	Bony	Manual alignment of the spine, sternum, and ribs using translations and rotations. All other registrations use translational degrees of freedom only	Manual
Standard NMI	Standard	Direct, automatic registration of lung cancer targets, including the primary tumor and/or involved lymph nodes, between on-treatment and planning images	Automatic
Seeded NMI	Seeded	Quick, approximate manual prealignment of targets, followed by standard registration	Semi-automatic
Intermediate transitive-based	Intermediate-TB	Alignment of on-treatment and planning images by composing the separate registrations of each to a single intermediate image [Eq. (2)]	Automatic
Consecutive transitive-based	Consecutive-TB	Alignment of on-treatment and planning images by composing the separate registrations between all consecutive weekly images [Eq. (3)]	Automatic
Intermediate rereferenced	Intermediate-RR	Designation of a single, intermediate weekly CT as the new reference for registration of all subsequent treatment fractions, given that the relative orientation is known between the new reference and planning images [Eq. (4)]	Semi-automatic
Consecutive rereferenced	Consecutive-RR	Designation of the previous weekly CT as the new reference for registration of the current on-treatment image, given that the relative orientation is known between the new reference and planning images [Eq. (5)]	Semi-automatic
Nominal centroid alignment	Centroid	Registration to minimize centroid localization errors for all targets simultaneously	Computed from target contours
Nominal border alignment	Border	Registration to minimize the distance between reference and secondary target borders in the left–right, anterior–posterior, and superior–inferior directions, computed directly from the manual contours	Computed from target contours

volume deformations. In the consecutive-TB strategy, each weekly CT was registered to the on-treatment image from the previous week. The relative orientation between secondary and reference images was then computed as the composition of all consecutive registrations, or

$$\mathbf{T}^{TB}_{\text{sequential}}(S_n \rightarrow R) = \mathbf{T}(S_2 \rightarrow R) \circ \mathbf{T}(S_3 \rightarrow S_2) \circ \ldots \circ \mathbf{T}(S_n \rightarrow S_{n-1}). \quad (3)$$

Each individual registration in this series exploited the greatest similarity of internal anatomy by matching sequential weekly CTs. However, the propagation of residual LE from each consecutive registration could also result in unacceptable target localization if not carefully controlled at each step. Both intermediate-TB and consecutive-TB registrations were considered fully automatic, as the composition of multiple registrations should not require manual interaction.

The final localization technique, termed "rereferenced" (RR) registration, was similar to the transitive-based strategy. Weekly images were still registered to an intermediate CT, but the intermediate CT was established as a new reference image for registration, requiring the relative orientation between new and original reference images to be determined (e.g., through offline review prior to the current treatment fraction). Specifically, this was accomplished by performing a nominal centroid alignment between contoured targets from the new and original reference images. Because this transform was known, it did not contribute to the propagation of residual target LE. As with TB registration, two subtypes of RR registration were explored. Intermediate-RR registration involved the registration of all weekly CTs acquired during or after the fourth week of treatment directly to the week 3 CT, given that the transformation between the week 3 CT and the reference image was known,

$$\mathbf{T}^{RR}_{\text{intermed}}(S_n \rightarrow R) = \begin{cases} \mathbf{T}_{\text{known}}(S_3 \rightarrow R) \circ \mathbf{T}(S_n \rightarrow S_3) & 3 < n \\ \mathbf{T}(S_n \rightarrow R) & 1 < n \leq 3 \end{cases}. \quad (4)$$

Consecutive-RR registration required that each weekly CT was registered directly to the on-treatment image from the previous week, given that the transformation between the previous weekly CT and the reference image was known,

$$\mathbf{T}^{RR}_{\text{sequential}}(S_n \rightarrow R) = \mathbf{T}_{\text{known}}(S_{n-1} \rightarrow R) \circ \mathbf{T}(S_n \rightarrow S_{n-1}). \quad (5)$$

In both cases, we assumed that manual interaction was necessary to determine the known transformations, resulting in semi-automatic registration techniques.

II.D. Simultaneous target registration

Because lung cancer targets are not typically treated as separate structures in planning, a single transformation was sought that simultaneously optimized the alignment of both the primary tumor and lymph nodes for treatment. Only, the fourteen patients presenting with both primary and lymph node GTVs were considered for this analysis. Two strategies were tested for localizing these two volumes concurrently. In the first method, termed "collective" registration, the GTV_P and GTV_{LN} were combined into a single structure for registration, but with LE determined for each target separately. The second method, referred to as "averaged" registration, involved separate registrations of the GTV_P and

GTV_{LN}, with a final transformation computed as the unweighted average of the two individual alignments. All registration strategies for individual target localization were also implemented for both collective and averaged simultaneous target alignment.

II.E. Data analysis

Evaluation of registration accuracy was based on target centroid and border LE. Centroid LE was defined as the displacement in the center-of-volume of secondary targets from that of the corresponding reference target. Because centroid LE may not be fully sufficient to characterize localization accuracy in cases of large target deformation and volume change,[29] target border LE was considered as an alternative metric. Border LE was defined as the shift of a secondary target border radially outward from the corresponding border of a reference structure in each of the cardinal directions: left–right (LR), anterior–posterior (AP), and superior–inferior (SI). A radially inward shift implied that the border of the secondary target was contained within the reference structure, resulting in an increased probability of adequate target coverage along that border. Therefore, only outward shifts were considered in this analysis, similar to the method used previously by Hugo *et al.*[33] A threshold of 2 mm for border LE was selected as a reasonable clinical action level, below which corrections would not be performed.[33] Because the number of targets with border LE varied among registration strategies, the mean border LE provided an inconsistent comparison. Instead, we compared the fraction of targets with border LE, defined as the percentage of all target borders with errors greater than the given threshold. For example, a value of 1 implied that all borders had LE greater than 2 mm, whereas a value of 0 indicated that no borders had LE exceeding 2 mm.

Using these error metrics, nominal registrations were determined to provide optimal target localization from the manually-delineated structures, as follows. First, nominal centroid alignments were computed as the transformation minimizing the displacement of target centroids, considering only translational degrees of freedom. The nominal centroid alignment for an individual target volume was given by perfectly overlapped centroids (i.e., LE of 0 mm) and was not considered for statistical analysis. For simultaneous target registration, all centroid displacements were minimized concurrently, yielding a nonzero error magnitude. Nominal border alignments were also performed to minimize the distance between reference and secondary target borders in the cardinal directions (i.e., along the LR, AP, and SI axes), again considering only translational degrees of freedom. Potentially nonzero border LE was possible for both individual and simultaneous nominal border alignment. Note that optimal centroid and border LE were determined from separate registrations. Also, because these nominal, contour-based registrations served only to determine the lower bound of each respective LE metric, it was not necessary to compute border LE for centroid alignment or centroid LE for border alignment.

To test for significant differences between various registration techniques, a one-way, repeated measures analysis of variance known as the Friedman test was performed for centroid LE. Because the centroid LE was non-normally distributed, this nonparametric test was chosen to perform analysis of variance using the ranks of centroid LE data across all registration techniques, providing a more conservative analysis than the corresponding parametric test. Intercomparisons between registration techniques were made using the Tukey range test. For individual target registration, this analysis was applied separately for GTV_P and GTV_{LN} centroid LE (Fig. 3), whereas for simultaneous target registration, a single analysis was applied over the centroid LE from both targets collectively (Fig. 5).

Studies have shown that target volume regression can compromise target shape and position reproducibility.[4,29,34] Linear regression was used to determine correlation of LE magnitude with regressing target volumes throughout treatment. Registrations were considered more robust against volume regression as the R^2 value decreased. In addition to these effects, pathology-induced changes, including atelectasis and pleural effusion, may affect tissue contrast adjacent to targets and impact the accuracy of rigid registration. In this study, five patients demonstrated atelectasis and two patients demonstrated pleural effusion, all of which either fully or partially resolved or progressed during treatment. To determine the significance of these effects, we compared the centroid LE for patients with and without pathology-induced changes using a Wilcoxon rank sum test. This nonparametric analysis was chosen to address the non-normal distribution of centroid LE. If patients with pathology-induced changes did not demonstrate centroid LE significantly greater than patients without such changes, then registrations were considered robust against this influence.

III. RESULTS

III.A. Individual target registration

Manual alignment of bony-anatomy resulted in initial centroid LE of 7.3 ± 5.4 mm for the GTV_P and 5.3 ± 3.4 mm for the GTV_{LN}. As shown in Fig. 2(a), bony alignment error demonstrated moderate correlation with the normalized primary tumor volume throughout treatment ($R^2 = 0.396$). This relationship was less evident for lymph nodes [Fig. 2(b), $R^2 = 0.197$]. In this initial alignment, patients with pathology-induced changes had mean GTV_P LE of 9.2 ± 6.9 mm, compared to 6.0 ± 3.7 mm for patients without these changes ($p = 0.10$). GTV_{LN} LE were 7.3 ± 3.6 mm and 3.5 ± 1.7 mm for patients with and without these changes, respectively ($p < 0.001$).

Automatic registration using the cross correlation algorithm increased centroid LE to 10.0 ± 8.5 mm and 6.9 ± 4.4 mm for the GTV_P and GTV_{LN}, respectively. Local correlation slightly reduced corresponding LE to 6.5 ± 5.5 mm and 4.8 ± 4.1 mm, but the NMI cost function provided the lowest absolute mean LE of 5.8 ± 6.0 mm and 3.2 ± 2.5 mm. NMI registration also reduced the correlation of centroid LE with normalized target volume throughout treatment (GTV_P, $R^2 = 0.203$;

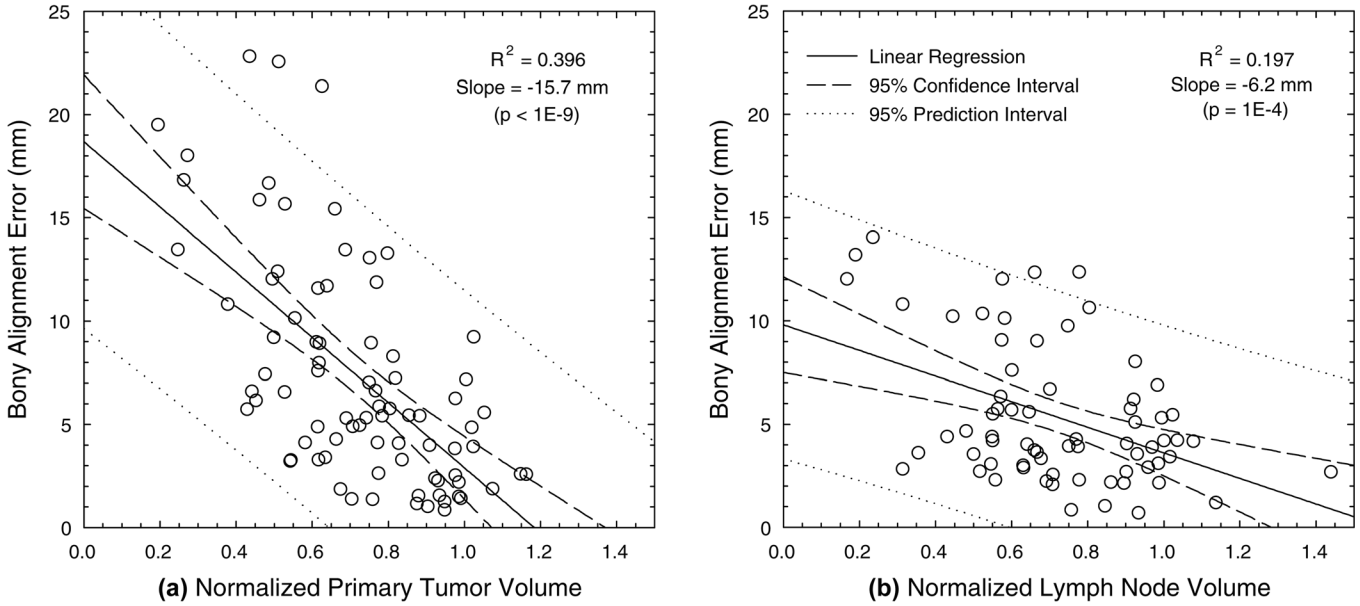

FIG. 2. Magnitude of centroid LE after manual bony-anatomy registration, plotted against the normalized target volume relative to the beginning of treatment for (a) the primary tumor and (b) involved lymph nodes.

GTV_{LN}, $R^2 = 0.080$). Patients with pathology-induced changes still demonstrated GTV_P LE approximately 1.5 times larger than patients without these changes ($p > 0.10$); however, the difference between GTV_{LN} LE was reduced to just 0.8 mm for these patient subgroups as a result of NMI registration ($p > 0.10$). Because NMI demonstrated the most potential to improve target localization, this similarity metric was used for all remaining studies.

Seeded NMI registration further improved centroid LE for both the GTV_P and GTV_{LN}, respectively (Table III and Fig. 3). The overall reduction in LE, however, stemmed from just a handful of registrations with substantially improved localization. Compared to standard NMI alignment, only 8 out of 82 seeded GTV_P registrations improved LE by more than 2 mm, but with an average improvement of 15.9 mm (range: 3.7–28.5 mm). Likewise, only 4 out of 69 seeded lymph node registrations improved LE, but with an average improvement of 7.1 mm (range: 2.8–10.5 mm). Large centroid LE persisted for remaining registrations, with 35% of GTV_P and 10% of GTV_{LN} registration errors still exceeding 5 mm. Despite these limitations, seeded registrations reduced the difference in centroid LE to just 0.5 mm between patient subgroups with and without pathology-induced changes ($p > 0.10$). The correlation between centroid LE and normalized target volume was also weak (GTV_P, $R^2 = 0.03$; GTV_{LN}, $R^2 = 0.11$).

Similar LE magnitudes were obtained from intermediate-TB and consecutive-TB registration techniques. Linear propagation of residual errors contributed to the magnitude of LE for these registrations. Rereferenced registrations demonstrated the lowest centroid LE for both targets in this study, although the improvements in target localization were much more pronounced for the GTV_P than the GTV_{LN}. As with seeded registrations, TB and RR registration strategies produced negligible differences in centroid LE between patient subgroups with and without pathology-induced changes for

TABLE III. Mean (standard deviation) of the magnitude of *centroid* LE for both individual target registration (GTV_P or GTV_{LN}) and simultaneous target registration (collective or averaged). "Collective" registration involved the simultaneous alignment of the GTV_P and GTV_{LN} using a single registration, whereas "averaged" registration consisted of separate alignments for each individual target volume, which were then averaged together to obtain the final transform.

		Primary tumor registration (mm)			Lymph node registration (mm)		
Registration	Short name	GTV_P	Collective	Averaged	GTV_{LN}	Collective	Averaged
Bony-anatomy	Bony	7.3 (5.4)	7.3 (5.7)	7.3 (5.7)	5.3 (3.4)	5.3 (3.4)	5.3 (3.4)
Standard NMI	Standard	5.8 (6.0)	6.7 (6.9)	5.7 (5.5)	3.2 (2.5)	4.9 (4.1)	4.0 (2.7)
Seeded NMI	Seeded	4.3 (2.5)	6.0 (6.1)	4.6 (3.1)	2.8 (1.8)	5.1 (4.4)	3.9 (2.3)
Intermediate transitive-based	Intermediate-TB	4.7 (3.7)	6.3 (7.2)	4.9 (4.2)	3.0 (2.0)	5.7 (5.0)	3.6 (2.1)
Consecutive transitive-based	Consecutive-TB	4.8 (3.7)	7.8 (12.3)	5.1 (3.8)	3.3 (1.7)	6.9 (10.7)	3.8 (2.2)
Intermediate rereferenced	Intermediate-RR	3.2 (3.0)	5.5 (5.8)	4.2 (3.3)	2.6 (2.2)	5.2 (4.3)	3.9 (2.5)
Consecutive rereferenced	Consecutive-RR	2.4 (2.1)	5.0 (5.2)	3.9 (2.7)	2.2 (1.4)	4.9 (3.7)	3.8 (2.3)
Nominal centroid alignment	Centroid	0.0 (0.0)	3.3 (2.3)	3.3 (2.3)	0.0 (0.0)	3.3 (2.3)	3.3 (2.3)

Note: GTV_P: primary gross tumor volume; GTV_{LN}: lymph node gross tumor volume; NMI: normalized mutual information algorithm.

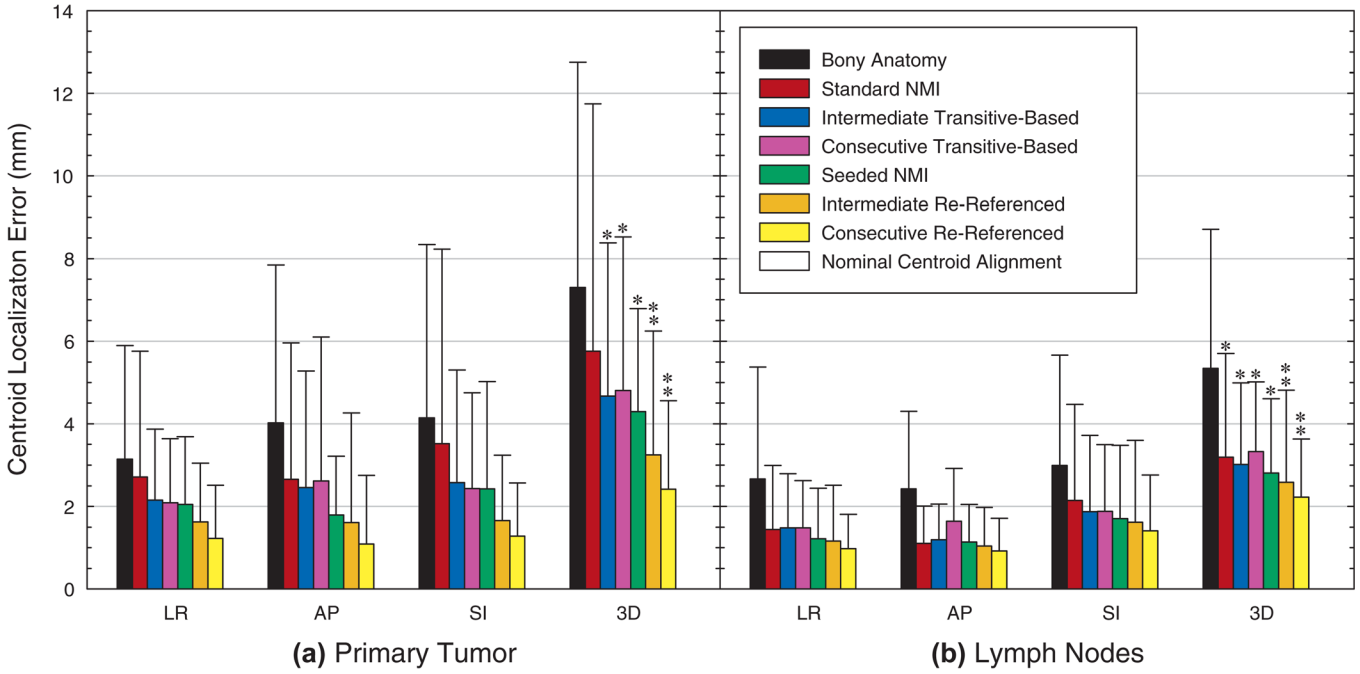

FIG. 3. Mean absolute centroid LE in the LR, AP, and SI directions and in three-dimensional (3D) magnitude after individual registration of (a) the primary tumor and (b) involved lymph nodes. Standard normalized mutual information (NMI) and transitive-based registrations were fully automatic, whereas seeded NMI and rereferenced registrations required varying degrees of manual interaction and were considered semi-automatic. Single asterisks denote significantly improved target localization relative to the initial bony-anatomy alignment, and double asterisks show additional significant improvement relative to other automatic registration techniques. Nominal centroid alignment of individual target volumes (GTV_P or GTV_{LN}) resulted in perfect centroid overlap, corresponding to zero centroid LE.

both the GTV_P ($p > 0.07$) and GTV_{LN} ($p > 0.10$). In addition, RR registrations were also robust against target volume regression, as the correlation between centroid LE and normalized target volume was largely eliminated (GTV_P, $R^2 \leq 0.07$; GTV_{LN}, $R^2 \leq 0.006$).

A Friedman test was used to compare initial bony alignment errors against centroid LE from individual target registration using the NMI algorithm (Table III). Significant LE reductions were observed for both the primary tumor ($p < 1 \times 10^{-9}$) and lymph nodes ($p < 1 \times 10^{-9}$). As shown in Fig. 3(a), all GTV_P registration techniques significantly improved primary tumor LE over bony alignment except for standard registration. In addition, rereferenced registrations demonstrated significant improvement over standard and transitive-based techniques. No significant difference was found between intermediate-RR and sequential-RR registrations. For the lymph nodes, all registration techniques provided significant improvement over bony alignment [Fig. 3(b)]. The consecutive-RR technique provided additional significant reductions over standard and transitive-based techniques but was not significantly better than seeded or intermediate-RR alignments.

Unlike centroid LE, the frequency of border LE greater than 2 mm, defined as the fraction of all target borders with LE greater than this threshold, demonstrated less substantial variation between different registration techniques (Table IV and Fig. 4). The frequency of GTV_P border LE decreased from 0.21 for bony alignment to between 0.12

TABLE IV. Fraction of all target borders demonstrating *border* LE greater than 2 mm for both individual target registration (GTV_P or GTV_{LN}) and simultaneous target registration (collective or averaged), as defined by the Table III caption.

		Primary tumor registration			Lymph node registration		
Registration	Short name	GTV_P	Collective	Averaged	GTV_{LN}	Collective	Averaged
Bony-anatomy	Bony	0.185	0.169	0.169	0.126	0.126	0.126
Standard NMI	Standard	0.152	0.169	0.133	0.082	0.140	0.106
Seeded NMI	Seeded	0.132	0.143	0.109	0.072	0.157	0.111
Intermediate transitive-based	Intermediate-TB	0.124	0.145	0.111	0.080	0.171	0.099
Consecutive transitive-based	Consecutive-TB	0.128	0.147	0.123	0.063	0.135	0.111
Intermediate rereferenced	Intermediate-RR	0.124	0.147	0.106	0.068	0.157	0.114
Consecutive rereferenced	Consecutive-RR	0.140	0.152	0.114	0.070	0.162	0.126
Nominal border alignment	Border	0.077	0.116	0.116	0.010	0.099	0.099

Note: GTV_P: primary gross tumor volume; GTV_{LN}: lymph node gross tumor volume; NMI: normalized mutual information algorithm.

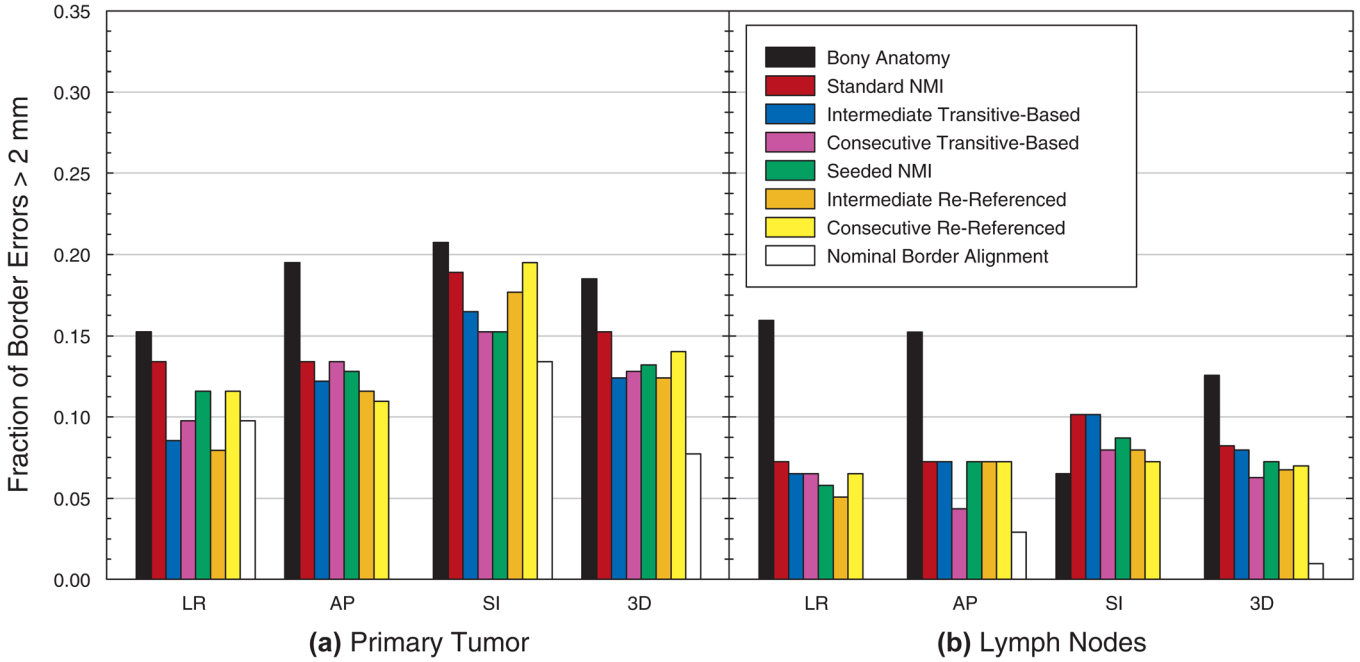

FIG. 4. Frequency of target border LE greater than 2 mm in the LR, AP, and SI directions and in all three dimensions (3D) after individual registration of (a) the primary tumor and (b) involved lymph nodes. Nominal border alignment was defined as the transformation that minimized localization errors for opposing target borders in each cardinal direction. In several cases, this provided localization of all borders in a given direction to within 2 mm, corresponding to a frequency of zero. NMI: normalized mutual information.

and 0.15 for the automatic and semi-automatic registration techniques. Nominal GTV_P border alignment indicated that border LE frequencies as low as 0.09 were possible. This nonzero frequency was attributed to target growth and shape change throughout treatment. For the GTV_{LN}, the frequency of border LE was reduced from 0.17 for bony alignment to between 0.06 and 0.08 for automatic and semi-automatic registration. Nominal border alignment showed that a frequency of 0.01 was possible for the lymph nodes.

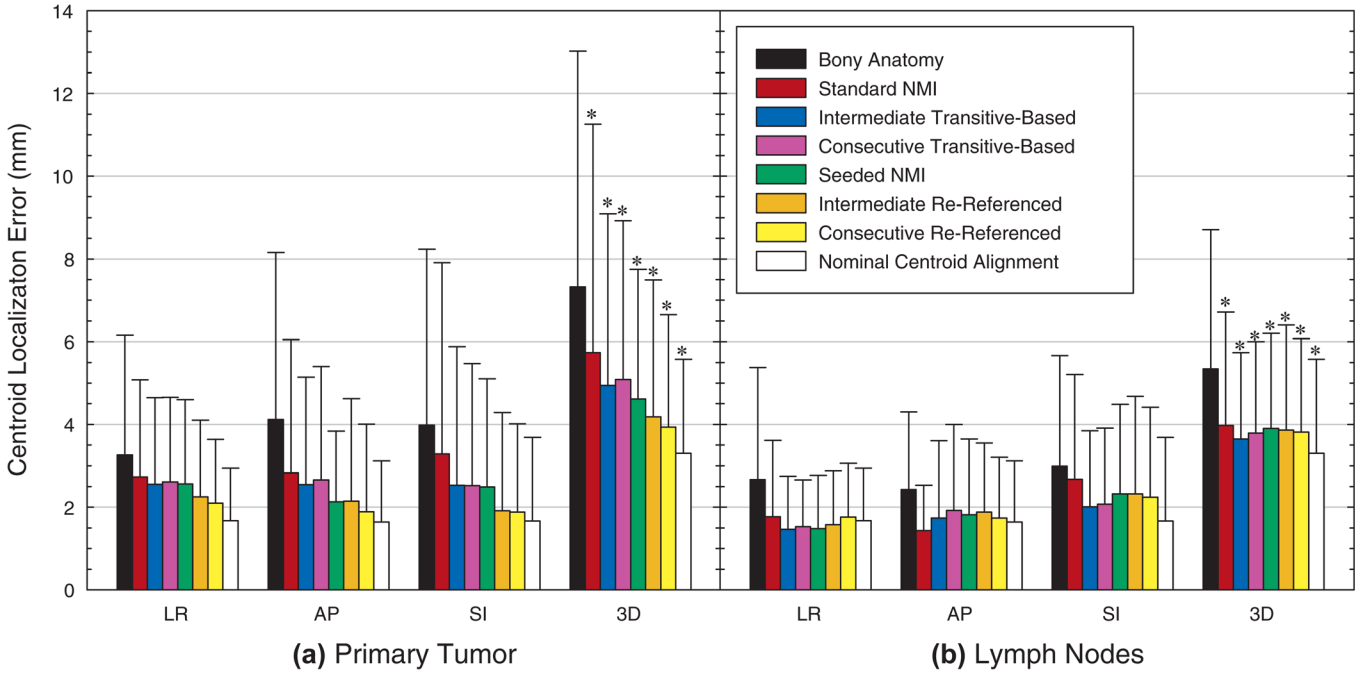

FIG. 5. Mean absolute centroid LE in the LR, AP, and SI directions and in three-dimensional magnitude (3D) after simultaneous "Averaged" registration of both the primary tumor and involved lymph nodes. This registration technique involved separate alignments of each individual target volume, which were then averaged together to obtain the final transform. Nominal centroid alignment was defined as the registration that minimized centroid LE for all targets simultaneously using only translational degrees of freedom, indicating the degree of intertarget variability throughout treatment. Asterisks denote significantly improved target localization relative to the initial bony-anatomy alignment. NMI: normalized mutual information.

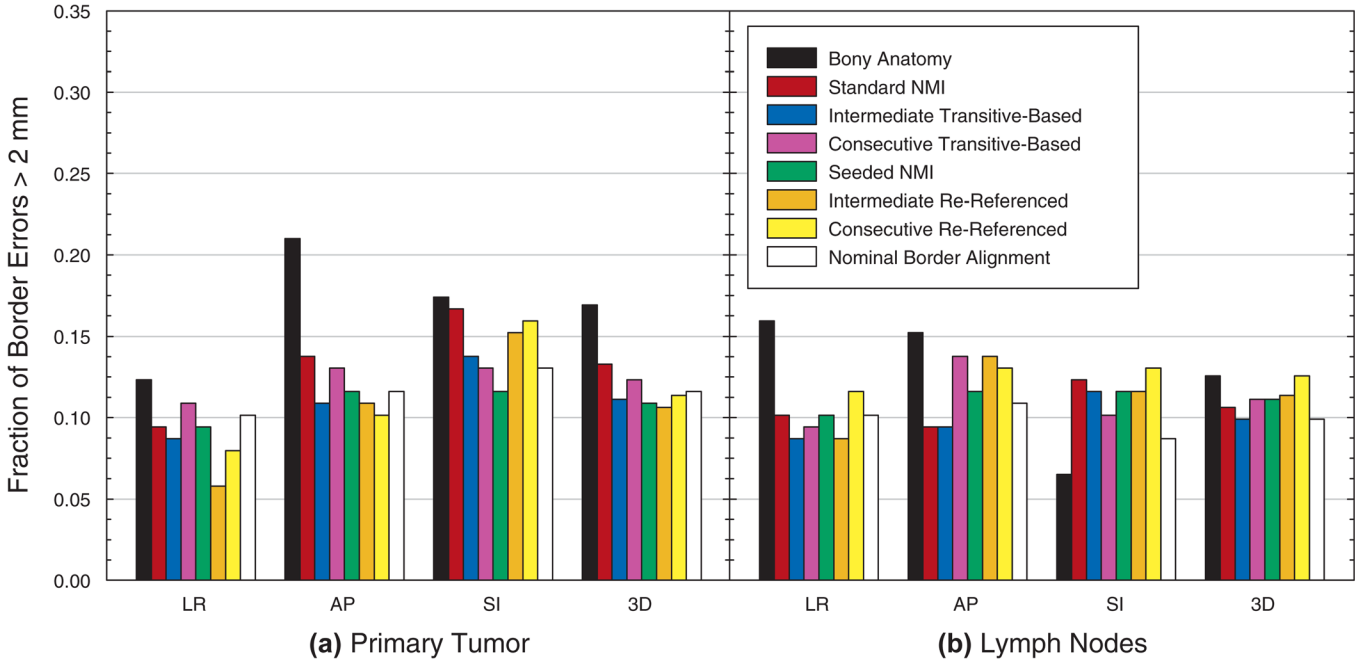

FIG. 6. Frequency of target border LE greater than 2 mm in the LR, AP, and SI directions and in all three dimensions (3D) after simultaneous "Averaged" registration of both the primary tumor and involved lymph nodes. This registration technique involved separate alignments of each individual target volume, which were then averaged together to obtain the final transform. Nominal border alignment was defined as the transformation that minimized localization errors for opposing target borders in each cardinal direction. NMI: normalized mutual information.

III.B. Simultaneous target registration

The collective method for simultaneous target registration demonstrated centroid LE ranging from 1.2 to 1.8 times greater than the corresponding averaged technique (Table III). Because averaged registrations consistently performed better for the current study population, this technique was exclusively chosen for further analysis. Figure 5 shows the mean absolute centroid LE for the primary tumor and involved lymph nodes using the averaged method of simultaneous target registration. Using a Friedman test, all automatic and semi-automatic registrations provided significant improvement over the initial bony alignment ($p < 0.020$). Consecutive-RR registration also reduced target centroid LE relative to standard registration by a significant margin ($p = 0.012$). Using nominal centroid alignment, minimum centroid LE of 3.3 ± 2.3 mm from manual target alignment was possible. These errors were significantly lower than all other registrations ($p < 0.012$) and provided an indication of intertarget variability throughout treatment.

In terms of border localization (Table IV, Fig. 6), the frequencies of border LE greater than 2 mm from bony alignment were 0.169 for the GTV_P and 0.126 for the GTV_{LN}. As with centroid LE, border LE frequencies were generally larger for collective registration than for averaged registration. The frequency of errors for averaged registration approached and in some cases surpassed the LE frequency from manual border alignment, generally at the expense of larger border LE for the other target. Seeded, averaged registration provided the most consistent border alignment, with frequencies of 0.11 for both targets. For comparison, minimum frequencies of 0.12 and 0.10 for the GTV_P and GTV_{LN}, respectively, were obtained from nominal border alignment.

IV. DISCUSSION

In this study, we aimed to evaluate the performance of rigid registration for localizing targets in locally-advanced lung cancer and to devise techniques to reduce LE for this task. Despite the use of active breathing control, the initial bony alignment resulted in large interfraction LE for the GTV_P, with systematic and random components consistent with those from other studies involving active breathing control.[29,34,35] Initial lymph node LE was also large and was comparable to centroid errors reported by Juhler-Nøttrup *et al.* from respiratory gated CTs acquired throughout treatment.[10] It was possible to reduce LE for both targets using automatic rigid registration. In particular, the NMI algorithm demonstrated better centroid alignment than either the local correlation or cross correlation algorithms. Significant improvements were observed for the GTV_{LN}; however, large GTV_P LE persisted, due in part to pathological and pathology-induced changes throughout treatment.

Seeded NMI registrations further reduced LE for the both targets. This strategy simulated a quick, approximate, manual pre-alignment of treatment targets performed by a clinician to guide the automatic registration. Although not a fully automated technique, manual pre-alignment of targets prior to automatic registration substantially improved 38% of GTV_P and 18% of GTV_{LN} cases having initial bony alignment errors greater than 10 mm. In addition, substantial improvements were demonstrated in 67% of both targets that had LE greater than 10 mm from standard registration.

A more profound improvement was noted for primary tumor localization, as only slight overall LE reductions were noted for the lymph nodes. In practice, no means exist to assess target LE during online image guidance, so this error threshold of 10 mm would be difficult to implement. Instead, clinician judgment would be required to gauge the necessity of seeding to guide automatic registrations.

Transitive-based registrations addressed the potentially large deformations observed in some patients but resulted in larger centroid LE than seeded registrations. Ideally, alignment of images acquired with fewer fractions between them should be more robust against such changes. Transitive-based registrations therefore resulted in the alignment of targets with increased similarity in size, shape, and configuration, which helped to reduce LE. In practice, during routine online guidance, intermediate-TB and consecutive-TB techniques only require a single registration between the on-treatment and intermediate images, as the relative orientation between intermediate and planning CTs will have been established during a previous treatment fraction. Therefore, transitive-based registration is no more costly than standard registration. One disadvantage of transitive-based registration, however, is the propagation of target LE.

While a quality assurance protocol should be an integral part of any automatic registration strategy, this would be especially important for transitive-based registration to avoid composing poor intermediate alignments.[36] Not only would this improve the localization of lung cancer targets but quality assurance may also prevent risk structures from entering treatment fields. For example, as Fig. 1 demonstrates, the correction of lymph node targets may induce large shifts in risk structures, potentially causing sensitive organs like the spinal cord and esophagus to be overdosed. It may be argued that automatic registration with quality assurance would overcomplicate the patient setup process, as an experienced therapist could provide adequate target alignment in a reasonable amount of time. However, for less experienced therapists, and for challenging patient cases (e.g., multiple targets, substantial pathological changes, or pathology-induced changes), an accurate automatic registration tool would greatly assist with target localization. Automatic registration may also improve the consistency of target localization, as manual alignments, including those performed by experts, are prone to some degree of variability.[16]

The most accurate target localization in this study was achieved using the intermediate-RR and consecutive-RR techniques. By establishing an intermediate weekly CT as the new reference for registration, transitive error propagation no longer impacted localization accuracy. The consequence, however, involved offline review to determine the relative orientation between new and original reference images. In the current study, this was accomplished by computing a nominal centroid alignment using existing target contours, which in practice would require recontouring of all target structures for each new reference image. As an alternative, new and original reference images could also be aligned using manual target localization[16] or deformable registration,[27,28] requiring the propagation of corresponding geometric uncertainties into the final LE. Because of the workload associated with rereferencing all intermediate images, consecutive-RR registration was considered too demanding for routine clinical protocols. Instead, we recommend intermediate-RR registration, particularly for patients with substantial target volume regression or pathology-induced changes.

The optimal week for rereferencing was found to be patient specific and difficult to predict *a priori*. The week 3 CT proved to be a reasonable intermediate image for most patients in the current study population, although this was not necessarily the optimal week for rereferencing. Both the normalized target volume and the time span between on-treatment and reference images were poor predictors of the potential improvement of rereferenced registration, relative to standard registration. However, rereferenced registration was considered robust against normalized target volume regression and provided insignificant LE differences between patient subgroups with and without pathology-induced changes. Therefore, establishing a new reference image may only be necessary for patients demonstrating these changes. Such a decision could be implemented as part of a quality assurance protocol. That is, if pathological or pathology-induced changes are observed to complicate automatic registration, centroid LE may be reduced by establishing the current on-treatment image as a new reference for subsequent fractions. More than one intermediate image may be necessary for patients with extraordinarily large deformations, as was the case for one patient whose GTV_P regressed 51% by week 3 and 81% by week 7. Replanning may be required to mitigate the dosimetric effect of such significant geometrical changes. This introduces the additional complication of target volume redefinition, as microscopic disease within the clinical target volume (CTV) may not necessarily demonstrate the same changes as the GTV. Rather than regenerating the CTV by expansion of each newly contoured GTV throughout treatment, the original CTV could be deformably propagated using the methods of Hugo *et al.*, thus preserving the original volume of soft-tissue for irradiation.[33] Note that recontouring does not necessarily imply replanning, as the orientation of each weekly image is ultimately determined relative to the original planning CT [Eqs. (4) and (5)]. Replanning may further improve treatment delivery but evaluating this hypothesis was outside the scope of the current study.

Prioritizing the alignment of primary tumors at the expense of lymph node targets produced substantial LE due to intertarget variability, consistent with findings from other studies.[18,37] This could lead to clinically relevant deviations in lymph node dose as well as increased dose to nearby risk structures.[38] Knap *et al.* reported that registration of the internal target volume (containing both the GTV_P and GTV_{LN}) was preferable to the alignment of bony-anatomy or individual targets.[39] However, even though collective registration tended to reduce centroid LE relative to bony alignment, large residual errors persisted for patients in this study. Better target localization was achieved by registering the primary tumor and lymph node targets separately, then computing the unweighted average of individual target registrations. Using

nominal centroid alignment based on target contours, minimum centroid LE exceeding 3 mm were observed due to differential variability between primary lung tumors and involved lymph nodes throughout treatment. This indicates that simple couch shifts were not sufficient to correct all interfractional geometric uncertainties.[16,37] Various adaptations of standard registration provided simultaneous target localization that approached this lower threshold, particularly using rereferenced registrations. Further reductions in centroid LE would likely require some form of adaptive radiotherapy, which could compensate for changes in target shape, volume, and configuration.

Coupling adaptation with optimal target localization techniques may provide a more efficient form of adaptive radiotherapy, where rereferenced registration and replanning are not required daily. For example, daily online replanning could theoretically reduce interfractional geometric uncertainties to near zero. However, online replanning remains an expensive process in terms of personnel, process costs, and the time each patient would spend on the treatment table. Instead, a high quality online registration could help to identify cases where replanning is required or where a simple online couch shift is sufficient for target localization. This would reduce the frequency of online replanning in many cases, improving the efficiency of the adaptive process. Furthermore, replanning implies the selection of a new reference image for registration of future fractions. This form of adaptation could therefore reduce the lower bound of target LE and minimize registration errors. More treatment fractions would rely on automatic registration, improving the efficiency of adaptive radiotherapy by reducing the necessary frequency of replanning.

One limitation of this study involved the registration of helical CT scans to simulate patient setup. More realistic clinical protocols would require registration between a planning CT and a cone-beam or megavoltage CT, in which image quality will differ. With cone-beam CT, no difference would be expected in the alignment of high-contrast boundaries between lung tumors and the surrounding lung parenchyma, but poor soft-tissue differentiation of mediastinal tumors and involved lymph nodes may increase LE and complicate registration techniques explored in the current study. Soft-tissue surrogates such as the carina may be necessary to assist with the localization of mediastinal targets from CBCT images. As such, the reader should consider the results of this study to be a lower bound on LE for lung cancer targets during image-guided radiotherapy. This also implies a lower limit on the required size of treatment margins. However, we refrain from computing margins for the current study population because only one source of uncertainty—interfractional geometric variability—was considered. Margin formulations are most useful only when they consider all sources of uncertainty throughout treatment.

As a second potential limitation, comparison of the various registration techniques was based solely on centroid and border LE for the GTV, which may not necessarily correlate with those of the CTV.[33] Optimal GTV localization may also place nearby critical structures at higher risk of irradiation, particularly for tumors demonstrating anisotropic regression. CTV and critical structure localization is the subject of future study. Despite the use of PINNACLE[3] as the only tested platform for data collection, the registration algorithms of this treatment planning system should be generalizable to other registration platforms as well. Finally, only translational degrees of freedom were used in this study to simulate couch shifts, but further improvements in target alignment may be possible by including rotations,[40] especially for simultaneous registration. All of these considerations are important to achieve optimal tumor coverage and normal tissue sparing.

V. CONCLUSIONS

Locally-advanced lung cancer presents a challenge to standard, rigid image registration due to target shape, volume, and configuration changes commonly observed in this disease. To improve target alignment with image-guided radiation therapy, periodically establishing a new reference image for automatic or semi-automatic registration is suggested, particularly for primary lung tumors. For simultaneous alignment of the primary tumor and involved lymph nodes, individual targets should be registered separately and the resulting transformations averaged, rather than aligning the collective volume of all targets with a single registration. Despite improvement in target alignment with these methods, intertarget variability limits the accuracy of simultaneous target registration, indicating that couch shifts cannot be used to correct all localization errors.

ACKNOWLEDGMENTS

The authors wish to thank Dr. Matthew Orton for assisting with delineation and Dr. Nitai Mukhopadhyay for verifying all statistical analyses. This work was partially supported by NIH R01CA116249. None of the authors has any actual or potential conflicts of interest.

[a]Author to whom correspondence should be addressed. Electronic mail: gdhugo@vcu.edu.; Telephone: 804-628-3457; Fax: 804-628-0271.

[1]J. Y. Chang *et al.*, "Image-guided radiation therapy for non-small cell lung cancer," J. Thorac. Oncol. **3**, 177–186 (2008).
[2]M. van Herk *et al.*, "The probability of correct target dosage: Dose-population histograms for deriving treatment margins in radiotherapy," Int. J. Radiat. Oncol., Biol., Phys. **47**, 1121–1135 (2000).
[3]G. K. Beckmann *et al.*, "How can we further improve radiotherapy for stage-III non-small-cell lung cancer?," Lung Cancer **45**, S125–S132 (2004).
[4]J.-J. Sonke and J. Belderbos, "Adaptive radiotherapy for lung cancer," Semin. Radiat. Oncol. **20**, 94–106 (2010).
[5]F.-M. Kong *et al.*, "High-dose radiation improved local tumor control and overall survival in patients with inoperable/unresectable non-small-cell lung cancer: Long-term results of a radiation dose escalation study," Int. J. Radiat. Oncol., Biol., Phys. **63**, 324–333 (2005).
[6]M. Partridge *et al.*, "Dose escalation for non-small cell lung cancer: analysis and modelling of published literature," Radiother. Oncol. **99**, 6–11 (2011).
[7]D. R. Simpson *et al.*, "A survey of image-guided radiation therapy use in the United States," Cancer **116**, 3953–3960 (2010).
[8]D. Verellen, M. D. Ridder, and G. Storme, "A (short) history of image-guided radiotherapy," Radiother. Oncol. **86**, 4–13 (2008).
[9]G. R. Borst *et al.*, "Kilo-voltage cone-beam computed tomography setup measurements for lung cancer patients; first clinical results and

comparison with electronic portal-imaging device," Int. J. Radiat. Oncol., Biol., Phys. **68**, 555–561 (2007).
[10]T. Juhler-Nøttrup *et al*., "Interfractional changes in tumour volume and position during entire radiotherapy courses for lung cancer with respiratory gating and image guidance," Acta Oncol. **47**, 1406–1413 (2008).
[11]L. A. Dawson and D. A. Jaffray, "Advances in image-guided radiation therapy," J. Clin. Oncol. **25**, 938–946 (2007).
[12]T. G. Purdie *et al*., "Cone-beam computed tomography for on-line image guidance of lung stereotactic radiotherapy: localization, verification, and intrafraction tumor position," Int. J. Radiat. Oncol., Biol., Phys. **68**, 243–252 (2007).
[13]I. S. Grills *et al*., "Image-guided radiotherapy via daily online cone-beam CT substantially reduces margin requirements for stereotactic lung radiotherapy," Int. J. Radiat. Oncol., Biol., Phys. **70**, 1045–1056 (2008).
[14]A. R. Yeung *et al*., "Tumor localization using cone-beam CT reduces setup margins in conventionally fractionated radiotherapy for lung tumors," Int. J. Radiat. Oncol., Biol., Phys. **74**, 1100–1107 (2009).
[15]G. D. Hugo *et al*., "Changes in the respiratory pattern during radiotherapy for cancer in the lung," Radiother. Oncol. **78**, 326–331 (2006).
[16]J. Higgins *et al*., "Comparison of spine, carina, and tumor as registration landmarks for volumetric image-guided lung radiotherapy," Int. J. Radiat. Oncol., Biol., Phys. **73**, 1404–1413 (2009).
[17]F. O. B. Spoelstra *et al*., "An evaluation of two internal surrogates for determining the three-dimensional position of peripheral lung tumors," Int. J. Radiat. Oncol., Biol., Phys. **74**, 623–629 (2009).
[18]E. D. Donnelly *et al*., "Assessment of intrafraction mediastinal and hilar lymph node movement and comparison to lung tumor motion using four-dimensional CT," Int. J. Radiat. Oncol., Biol., Phys. **69**, 580–588 (2007).
[19]J. Higgins *et al*., "Effect of image-guidance frequency on geometric accuracy and setup margins in radiotherapy for locally advanced lung cancer," Int. J. Radiat. Oncol., Biol., Phys. **80**, 1330–1337 (2011).
[20]K. R. Britton *et al*., "Assessment of gross tumor volume regression and motion changes during radiotherapy for non-small-cell lung cancer as measured by four-dimensional computed tomography," Int. J. Radiat. Oncol., Biol., Phys. **68**, 1036–1046 (2007).
[21]S. C. Erridge *et al*., "Portal imaging to assess set-up errors, tumor motion and tumor shrinkage during conformal radiotherapy of non-small cell lung cancer," Radiother. Oncol. **66**, 75–85 (2003).
[22]P. A. Kupelian *et al*., "Serial megavoltage CT imaging during external beam radiotherapy for non-small-cell lung cancer: Observations on tumor regression during treatment," Int. J. Radiat. Oncol., Biol., Phys. **63**, 1024–1028 (2005).
[23]G. Lim *et al*., "Tumor regression and positional changes in non-small cell lung cancer during radical radiotherapy," J. Thorac. Oncol. **6**, 531–536 (2011).
[24]M. L. Siker, W. A. Tomé, and M. P. Mehta, "Tumor volume changes on serial imaging with megavoltage CT for non-small-cell lung cancer during intensity-modulated radiotherapy: How reliable, consistent, and meaningful is the effect?," Int. J. Radiat. Oncol., Biol., Phys. **66**, 135–141 (2006).
[25]G. Bosmans *et al*., "Time trends in nodal volumes and motion during radiotherapy for patients with stage III non-small-cell lung cancer," Int. J. Radiat. Oncol., Biol., Phys. **71**, 139–144 (2008).
[26]J. R. Pantarotto *et al*., "Motion analysis of 100 mediastinal lymph nodes: Potential pitfalls in treatment planning and adaptive strategies," Int. J. Radiat. Oncol., Biol., Phys. **74**, 1092–1099 (2009).
[27]M. Guckenberger *et al*., "Evolution of surface-based deformable image registration for adaptive radiotherapy of non-small cell lung cancer (NSCLC)," Radiat. Oncol. **4**, 68 (2009).
[28]K. K. Brock *et al*., "Improving image-guided target localization through deformable registration," Acta Oncol. **47**, 1279–1285 (2008).
[29]C. K. Glide-Hurst, E. Gopan, and G. D. Hugo, "Anatomic and pathologic variability during radiotherapy for a hybrid active breath-hold gating technique," Int. J. Radiat. Oncol., Biol., Phys. **77**, 910–917 (2010).
[30]O. Škrinjar, A. Bistoquet, and H. Tagare, "Symmetric and transitive registration of image sequences," Int. J. Biomed. Imaging **2008**, 1–9 (2008).
[31]R. W. M. Underberg *et al*., "Time trends in target volumes for stage I non-small-cell lung cancer after stereotactic radiotherapy," Int. J. Radiat. Oncol., Biol., Phys. **64**, 1221–1228 (2006).
[32]C. Woodford *et al*., "Adaptive radiotherapy planning on decreasing gross tumor volumes as seen on megavoltage computed tomography images," Int. J. Radiat. Oncol., Biol., Phys. **69**, 1316–1322 (2007).
[33]G. D. Hugo *et al*., "Localization accuracy of the clinical target volume during image-guided radiotherapy of lung cancer," Int. J. Radiat. Oncol., Biol., Phys. **81**, 560–567 (2011).
[34]N. Panakis *et al*., "Defining the margins in the radical radiotherapy of non-small cell lung cancer (NSCLC) with active breathing control (ABC) and the effect on physical lung parameters," Radiother. Oncol. **87**, 65–73 (2008).
[35]J. Brock *et al*., "The use of the active breathing coordinator throughout radical non-small-cell lung cancer (NSCLC) radiotherapy," Int. J. Radiat. Oncol., Biol., Phys. **81**, 369–375 (2011).
[36]M. Sharpe and K. K. Brock, "Quality assurance of serial 3D image registration, fusion, and segmentation," Int. J. Radiat. Oncol., Biol., Phys. **71**, S33–S37 (2008).
[37]J.-J. Sonke, J. Lebesque, and M. van Herk, "Variability of four-dimensional computed tomography patient models," Int. J. Radiat. Oncol., Biol., Phys. **70**, 590–598 (2008).
[38]W. van Elmpt *et al*., "Should patient setup in lung cancer be based on the primary tumor? An analysis of tumor coverage and normal tissue dose using repeated positron emission tomography/computed tomography imaging," Int. J. Radiat. Oncol., Biol., Phys. (in press).
[39]M. M. Knap *et al*., "Daily cone-beam computed tomography used to determine tumour shrinkage and localisation in lung cancer patients," Acta Oncol. **49**, 1077–1084 (2010).
[40]M. Guckenberger *et al*., "Magnitude and clinical relevance of translational and rotational patient setup errors: A cone-beam CT study," Int. J. Radiat. Oncol., Biol., Phys. **65**, 934–942 (2006).